JMEPEG (2012) 21:508–515
DOI: 10.1007/s11665-011-9938-8

1059-9495/$19.00

Phase Evolution in Boride-Based Cermets and Reaction Bonding onto Plain Low Carbon Steel Substrate

B. Palanisamy and A. Upadhyaya

(Submitted September 16, 2010; in revised form February 2, 2011)

Reaction sinter bonding is a process that aims to bond two materials for improvement in properties through reactive sintering technique. The process has been effectively used to sinter hard materials like borides in situ which not only possess excellent oxidation resistance, good corrosion resistance but also resistant to abrasive wear. Sinter bonding is a unique surface modification process achieved through powder metallurgy and is competent with other techniques like boronizing sintering and sinter-brazing since it eliminates the additional operations of heat treatment and assembly and removes the inherent setbacks with these processes. This study focuses on identifying the phase evolution mechanism using characterization tools like x-ray diffractometry and energy dispersive spectroscopy and study of sinter bonding of the boron containing precursors (Mo-Cr-Fe-Ni-FeB-MoB) onto plain carbon steel. A microstructure containing Fe-based matrix dispersed with complex borides develops with temperature in the tape cast sheets. A fivefold increase in hardness between plain carbon steel in wrought condition and sinter bonded steel was observed. The multilayer consisted of a reaction zone adjacent to the interface and was investigated with the composition profile and hardness measurements. A model of sinter bonding between the cermet and the steel has also been proposed.

Keywords cermet, inter-diffusion, reaction bonding, sinter bonding, ternary boride

1. Introduction

Boride-based cermets are a new class of materials successfully being used for high-temperature wear applications like hot copper extrusion dies, powder/plastic injection molding equipment, pump impellers, etc. (Ref 1, 2). Borides inherently have high hardness (1600-1900 HV), transverse rupture strength (~2000 MPa) in cermet form and good oxidation resistance that make them suitable for demanding applications (Ref 3, 4). The material is consolidated through liquid phase sintering (Ref 5) and has a structure that contains hard dispersoids in a ductile metallic matrix. The sintering mechanism discussed elsewhere is similar to liquid phase sintering technique. The solution reprecipitation stage is highlighted here. The difficulties in consolidation of hard materials like borides owing to high wetting angles between boride and liquid phase are overcome by reactive sintering techniques. Reaction sintering combined with liquid phase sintering allows production of a densified microstructure in which a soft metallic matrix contains dispersed hard phases. The properties of Mo_2FeB_2-based hard alloys strongly depend not only on atomic ratio but also on its chromium content. It was reported that with increasing chromium substitution for molybdenum in the alloy the liquid formation is offset to higher temperatures from 1200 to 1300 °C for different chromium additions (Ref 6). Studies on Mo-Fe-B alloys clearly reveal that the densification rate is little affected by Mo addition up to 3 wt.% in contrast to boron. Molybdenum stabilizes the ferrite phase and the diffusion rate is significantly faster in ferrite as compared to the austenitic phase. Boron addition significantly enhances the densification kinetics. It forms a low melting (iron-rich boride Fe_2B in Fe) eutectic liquid phase. Consequently, the inter-particle voids are eliminated through capillary induced infiltration of this liquid (Ref 7). The high strength associated with the boride cermet microstructure has been discussed extensively elsewhere (Ref 4) and was attributed to the Cr and V additions which provided a homogenous distribution of the hard phase. The effect of various alloying elements was studied in detail and vanadium addition was reported to improve the transverse rupture strength considerably (Ref 8). The advantages of the sinter bonding process are that sophisticated equipment is unnecessary and also eliminate the need for additional heat treatment steps carried out in conventional surface treatment techniques. The process is unique in the aspect that the surface modification is achieved through powder metallurgy. The ideal sinter bonding temperature was found by differential thermal analysis and dilatometric analysis by Sivaraman et al. (Ref 9). It was observed that surface roughness had minor effect on bond strength. The bonding was carried out by a small application of load during sintering to enhance the bonding. A remnant interface was observed between the cermet and the steel after bonding (Ref 9). Rao and Upadhyaya (Ref 10) modified the sinter bonding process further to provide SiC reinforcements

B. Palanisamy and **A. Upadhyaya,** Department of Materials and Metallurgical Engineering, Indian Institute of Technology, Kanpur 208016, UP, India. Contact e-mail: barathp@gmail.com.

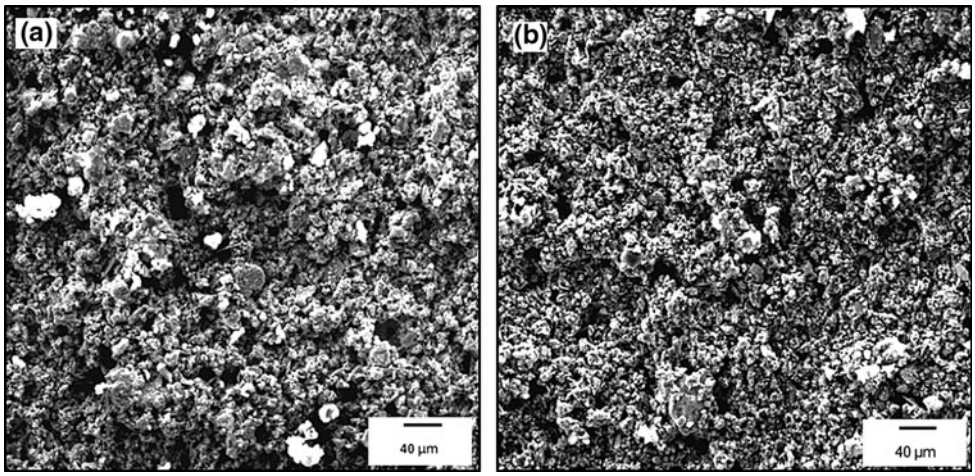

Fig. 1 Scanning electron micrograph of the as-received precursor (tape cast) sheets showing the powder

Table 1 Composition of boride precursor sheets in as-received tape cast condition

	Composition, wt.%				
Grade	**B**	**Mo**	**Cr**	**Ni**	**Fe**
C50	5	42.7	10.2	2.8	39.3
V30	5.4	46.6	1.9	2.9	43.2

within the bonded structure and an increase in transverse rupture strength was reported. The potential of this material for its use in the other applications is yet to be fully appreciated.

2. Materials and Methods

The boride-based precursor sheets (C50 and V30) were obtained from Toyo Kohan Ltd., Japan in the form of tape cast green sheets. The procedure for production is detailed elsewhere (Ref 11). Powders of Fe, Mo, Cr, and boron in combined form as FeB and MoB were premixed using organic binders poly vinyl butyral (PVB) and di-butyl phthalate (DBP) with 50 vol.% and cast into thin sheets of thickness 490 and 650 μm. Figure 1(a) (C50) and (b) (V30) shows the uniformly distributed microstructure and morphology of the constituents with the organic binder.

The boride precursors are broadly classified into Cr-rich sheet (C50) and Cr-lean sheet (V30) the composition of which is shown in Table 1.

Sintering of the precursor sheets and their sinter bonding onto the AISI 1018 (Fe 0.18 wt.% C) low carbon steel were carried out in flowing dry hydrogen atmosphere (dry H_2, dew point −35 °C) in a tubular furnace (OKAY 70T 7, Bysakh and Company, Kolkata) at a constant heating rate of 5 °C/min. The tape cast sheets were cycled from 700 to 1250 °C and the corresponding effects of temperature on density, microstructure, and phase evolution were evaluated. The samples were isothermally held at 1250 °C for 30 min for sinter bonding to occur with application of a constant load at high temperature to improve the surface contact between precursor sheets and the substrate. During sinter bonding cycle an intermittent hold of

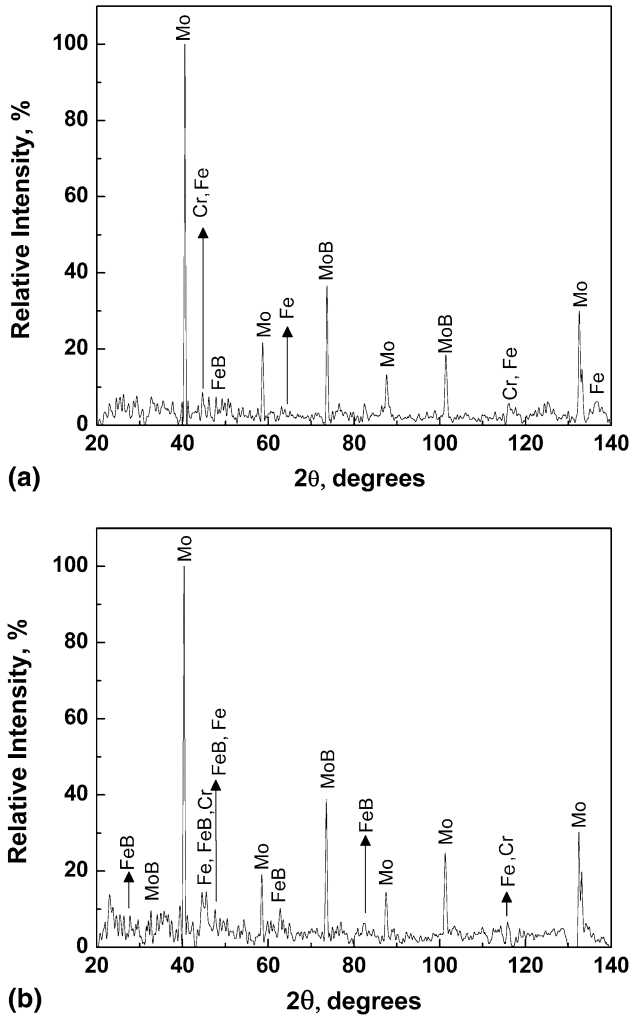

Fig. 2 XRD phase analysis of (a) C50 and (b) V30 precursor sheets in as-received condition

30 min was carried out for complete removal of the polymer-based binders. The electron micrographs and energy dispersive spectroscopy (EDS) of the metallographically prepared samples were obtained using scanning electron microscopy operating at

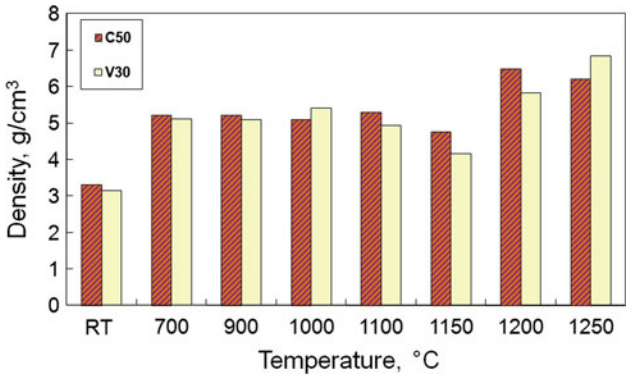

Fig. 3 Effect of temperature on the density of C50 and V30 sintered sheets

Table 2 Effect of temperature on the linear dimensional change (along thickness direction) of boride based cermets

Temperature, °C	Grade	Linear shrinkage, %
900	C50	0.15
	V30	0.13
1000	C50	7.04
	V30	4.32
1200	C50	10.37
	V30	3.66
1250	C50	0.06
	V30	2.71

20 kV (QUANTA 200 HV, FEI, Oregon, USA). The x-ray diffraction measurements were performed using x-ray powder diffractometer (ISO-Debyeflex 2002, Rich Seifert & Co., Germany) using Cu-K_α radiation (with $\lambda = 1.54$ Å) at a scan rate of 3 (°/min). The sinter bonded steel was sectioned using diamond wheel cutter and the microhardness was subsequently measured using microhardness tester (V TEST, Bareiss, Germany) at 50 g loads.

3. Results and Discussion

The various constituents present in the as-received condition of the tape cast sheets C50 and V30 were identified using x-ray diffraction technique and is shown in Fig. 2. The diffractograph is marked by elemental phases Fe, Mo, and Cr as well as binary borides of Fe and Mo.

During reaction bonding, it has been observed that high shrinkage occurs at around 1050 °C when the primary liquid phase solidifies and reaches a maximum as the secondary liquid phase solidifies consistent with data shown in Fig. 3. Table 2 shows the linear shrinkage up to 1250 °C.

Sintered density is found to increase monotonically for C50 and V30 as temperature increases, depicted in Fig. 3. This results in a more densified structure at higher temperatures owing to faster diffusion rates. The microstructure evolution of the boride sheets as sintering temperature increases is shown in Fig. 4 for both cermets.

As temperature is increased to 700 °C the polymer binder gets evaporated completely. Change in morphology of the particles begins to occur at this temperature and as temperature

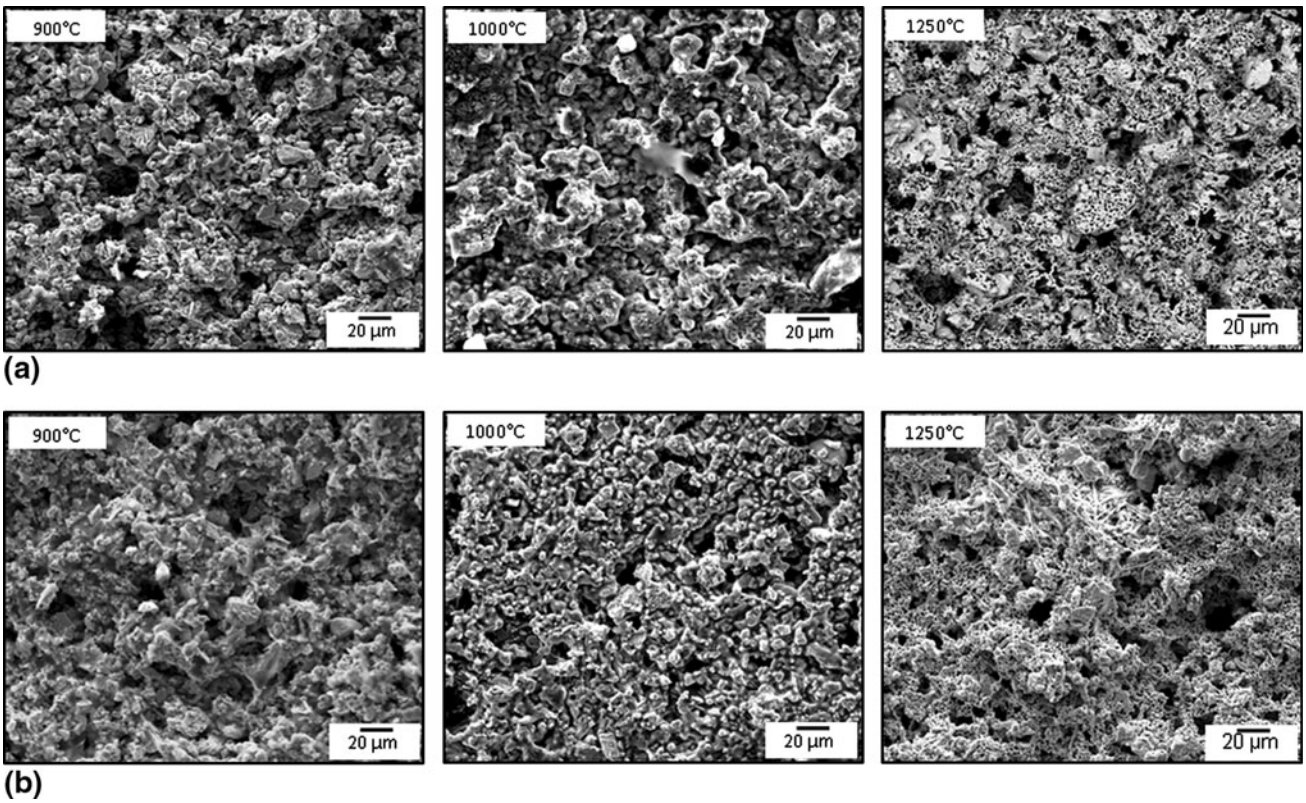

Fig. 4 Microstructural evolution with temperature (a) C50 boride-based cermet (b) V30 boride-based cermet

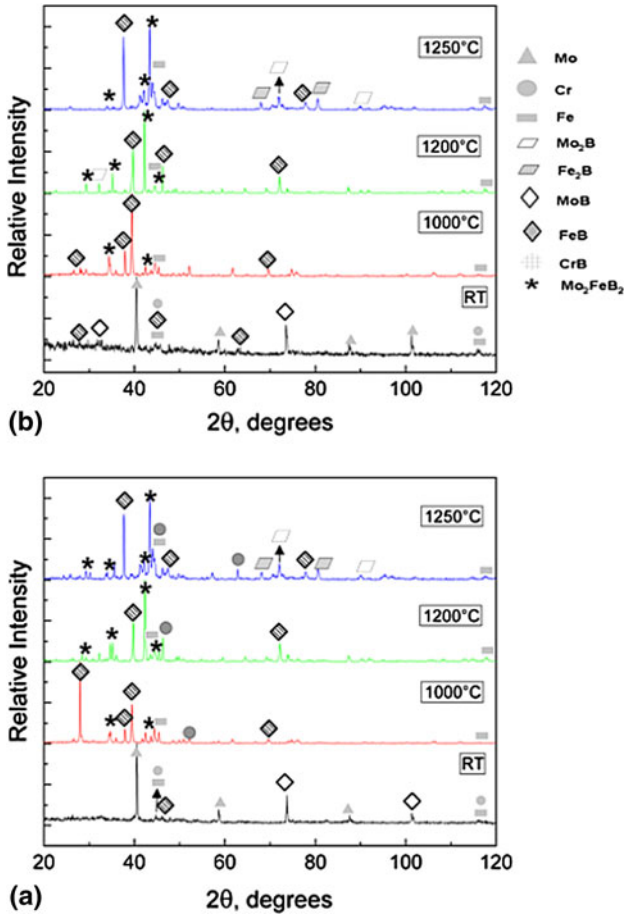

Fig. 5 Effect of sintering temperature on the phase evolution in (a) C50 and (b) V30 sheets

increases to 900 °C a networked structure begins to form. The material is still porous at these temperatures. The microstructure is similar in both C50 and V30 up to this point. A liquid phase begins to form at 1000 °C in the case of C50 cermet and at a slightly higher temperature in the case of V30 cermet. Lower porosity and higher interconnectivity are marked here. The complex boride phase Mo_2FeB_2 begins to form as temperature is increased beyond 900 °C and its presence is noted as precipitates with irregular morphology. This phase is expected to form during reaction sintering of the cermet as concluded in prior research (Ref 4, 12), the key difference in this case is that the occurrence of this phase has been detected at lower temperatures as found using x-ray diffraction data.

The desired microstructure of borides dispersed in a Fe-based matrix evolves as the material is heated above 1150 °C for C50 and at 1200 °C in the case of V30.

Phase analysis by x-ray diffraction technique (Ref 13) shows that elemental peaks of Fe, Mo, and Cr are observed along with boron sources FeB (orthorhombic) and MoB (tetragonal) at room temperature. The reaction initiates early in the V30 material marked by the occurrence of the hard phase Mo_2FeB_2 (tetragonal) which occurs only at 1000 °C in C50 and tetragonal Fe_2B phase which forms in C50 material. Residual unreacted phases of MoB are found in addition to Mo_2B and Fe_2B in both C50 and V30 precursor materials as temperature is increased to 1250 °C. As temperature increases, the elemental peaks except of Fe are replaced by peaks of boride precipitates (Fig. 5).

Based on the phase analysis the sequence of the various phenomena occurring during reaction sintering of the boride precursor sheets is summarized below.

At room temperature in chromium-rich C50 sheet the presence of elemental phases Fe, Cr, Ni, Mo is observed. Boron

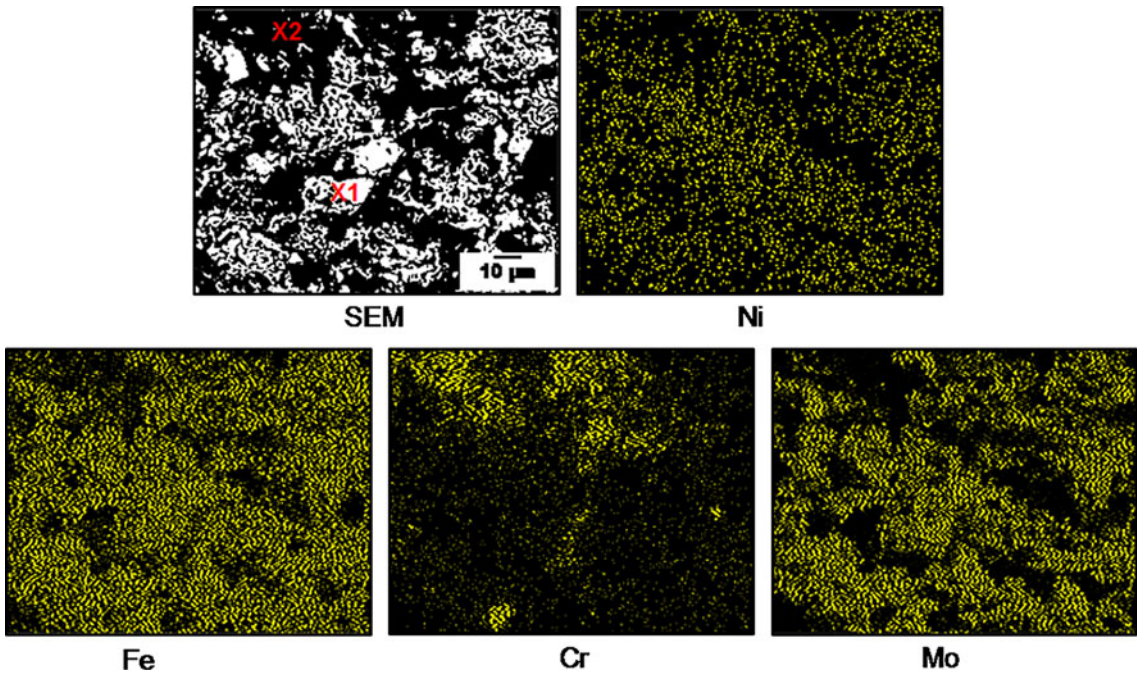

Fig. 6 Elemental distribution of constituents in C50 sheets sintered at 1250 °C

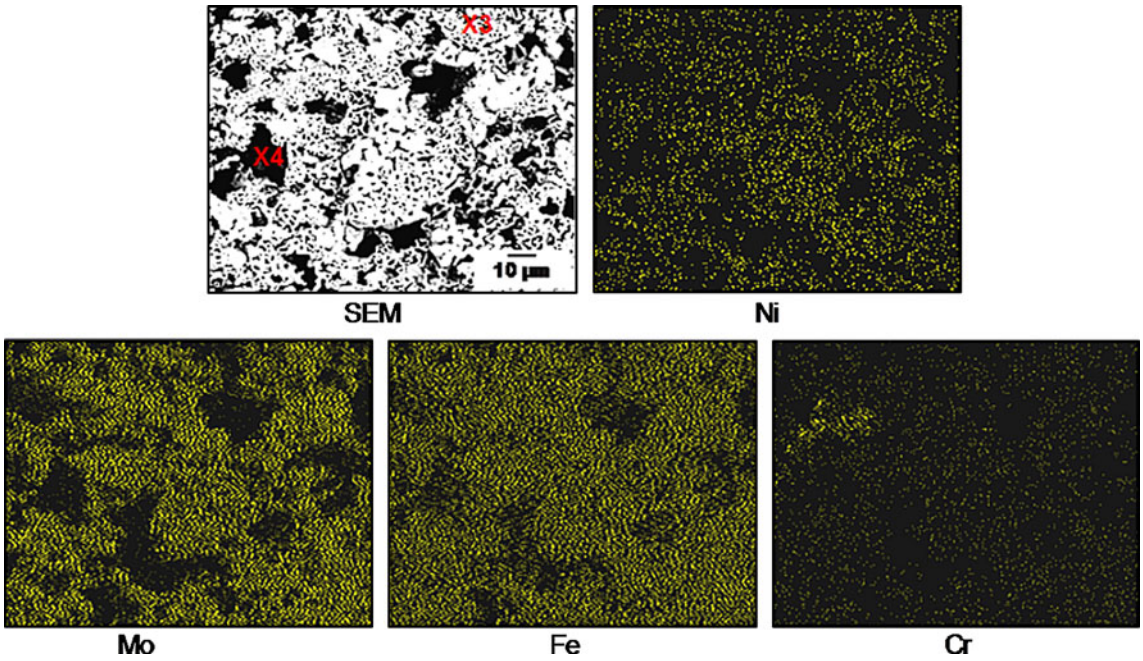

Fig. 7 Elemental distribution of constituents in V30 sheets sintered at 1250 °C

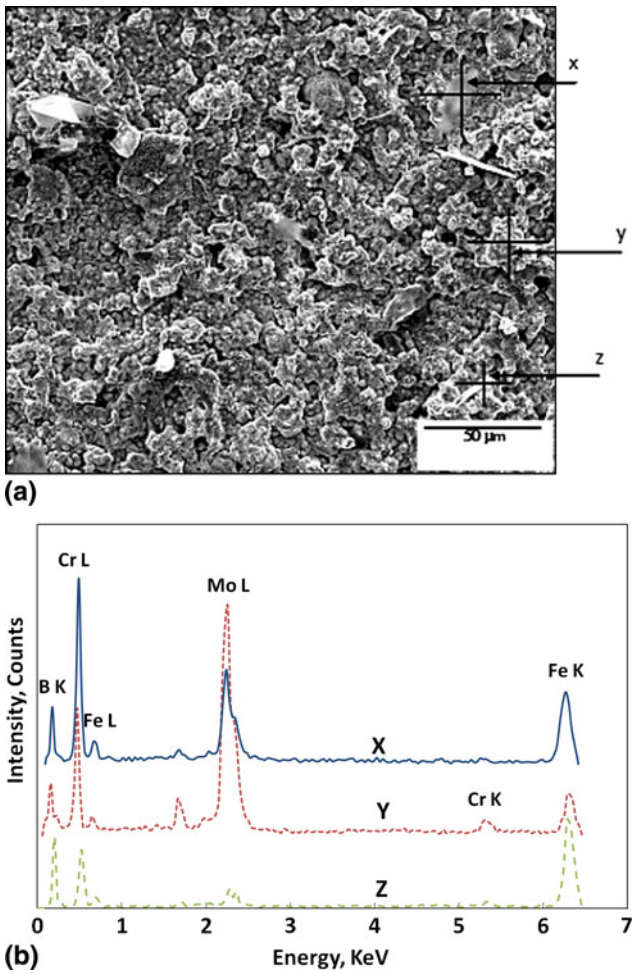

Fig. 8 (a) Microstructure of C50 cermet sintered at 1000 °C and (b) EDS on the spots indicated in (a)

is in combined form and is indicated by presence of FeB and MoB. At 1000 °C, the formation of FeB-rich L_1 phase occurs. In addition, there is also some evidence of CrB formation and precipitation of Mo_2FeB_2 phase. The L_1 phase is transient and as it reacts with MoB it results in formation of complex Mo_2FeB_2 phase. It is to be noted that CrB phase starts to form at 1000 °C and dissolves in to L_2 phase at 1200 °C onwards. As temperature rises to 1200 °C the formation of L_2 phase of permanent nature which is Fe-rich occurs. Now, the already coarsened Mo_2FeB_2 phase starts to dissolve into L_2 phase along with CrB. The presence of some other borides as well is observed which are basically Mo_2B and Fe_2B. When the peak sintering temperature of 1250 °C is attained the precipitation of fine, complex, quaternary boride $(Mo, Fe, Cr)_3B_2$ occurs. This stoichiometry is reported to form as a result of Cr dissolution in to the complex boride by Takagi et al. (Ref 1). The depleted L_2 then crystallizes in to the Fe-rich matrix alloyed with Mo, Cr, and Ni. Besides, the other borides (Mo_2B and Fe_2B) also seem to persist even when cooled to room temperature.

In the case of chromium-lean V30 sheet at room temperature we again have elemental phases Fe, Cr, Ni, Mo along with FeB and MoB. As temperature is raised to 1000 °C the observed phase transformation is very much similar to that of the C50 cermet and is marked by the appearance of L_1 and Mo_2FeB_2 phases at this temperature. Due to low Cr content no CrB phase formation occurs at any temperature. Cr goes into the solution and remains alloyed with the matrix. Further, at 1200 °C Fe-rich L_2 phase (permanent) is formed. In addition, the already coarsened Mo_2FeB_2 phase starts to dissolve into L_2 phase. The final microstructure consists of reprecipitated fine Mo_2FeB_2 in an alloyed Fe matrix which crystallizes from the L_2 phase. The existence of L_1 and L_2 has already been proven using dilatometric studies and x-ray diffraction in prior research (Ref 9). These phases form in both sintering of plain cermets as well as in sinter bonding. The temperature of formation of the liquid phase can be altered by varying the substrate steel composition.

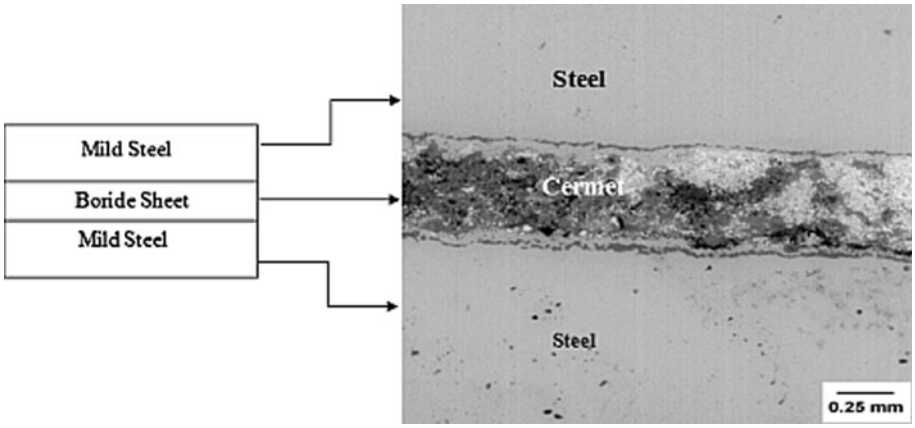

Fig. 9 Schematic of arrangement of boride sheet sandwiched between mild steel substrates (b) Photograph of the reaction bonded material with the same configuration as shown schematically in (a)

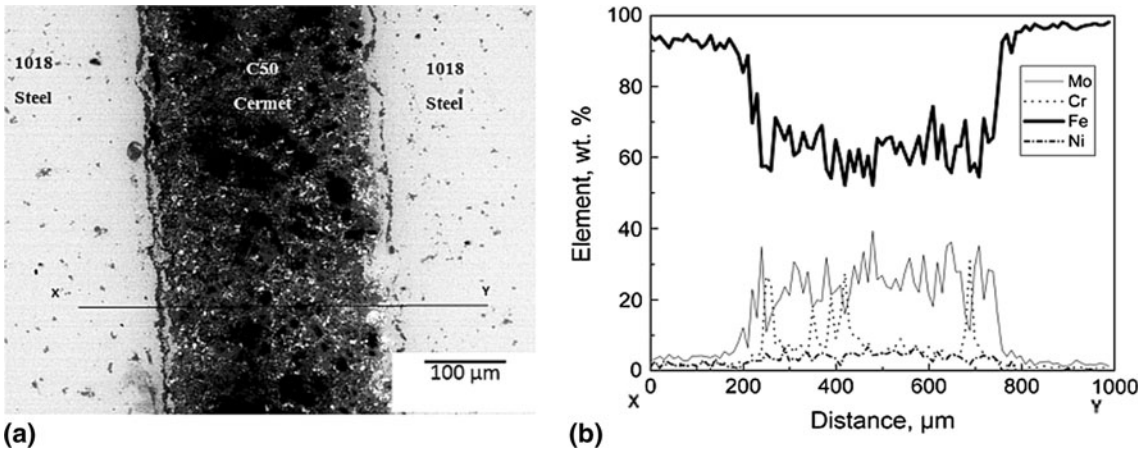

Fig. 10 SEM image of showing steel-cermet-steel interface in C50 cermet bonded onto 1018 steel. The line scan was performed from *X* to *Y* in the multilayer using EDS

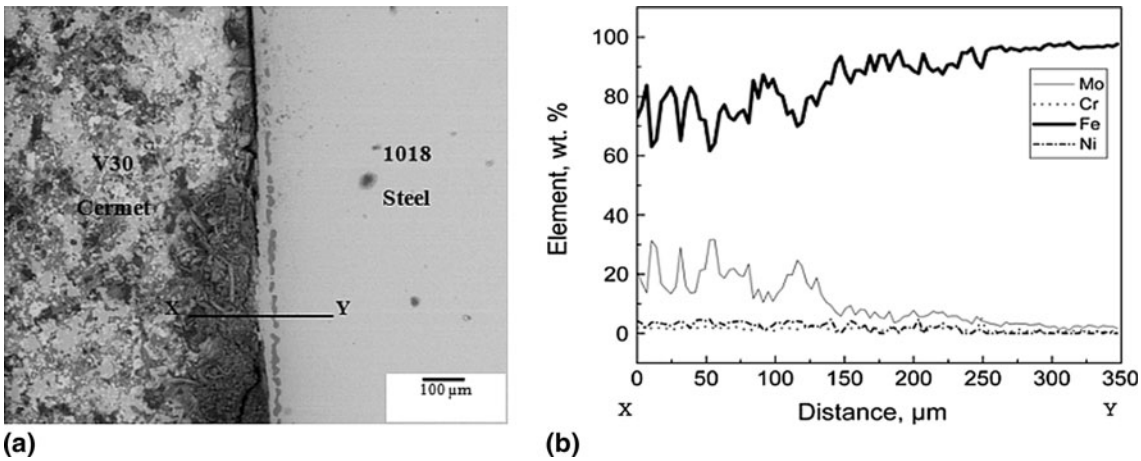

Fig. 11 Elemental line scan against cermet-steel interface for V30 cermet bonded onto 1018 steel

X-ray elemental map on the microstructure reveals the elemental distribution. This was carried out on cermet sheets sintered at 1250 °C and is shown in Fig. 6, 7. The elemental mapping technique provides some insights of distribution of the various elements in the microstructure of the sintered sheets.

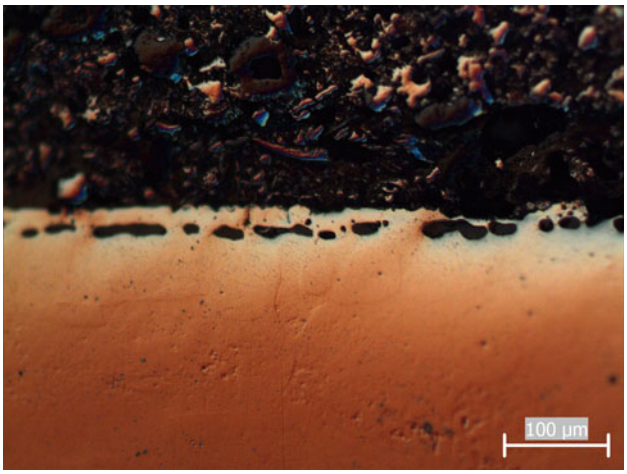

Fig. 12 Optical micrograph of interface between V30 cermet and 1018 steel substrate

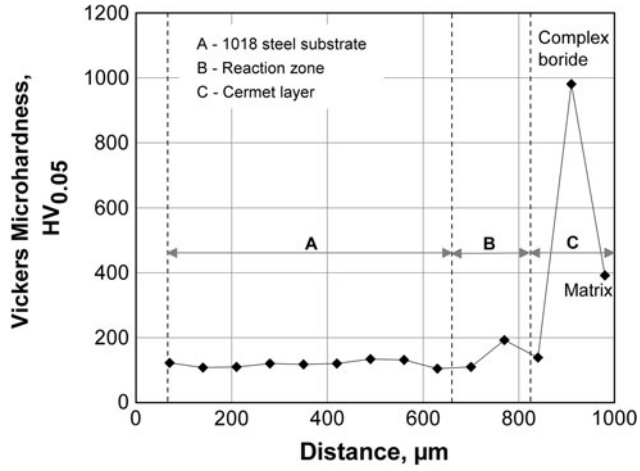

Fig. 14 Microhardness profiling across substrate-reaction zone-cermet multilayer

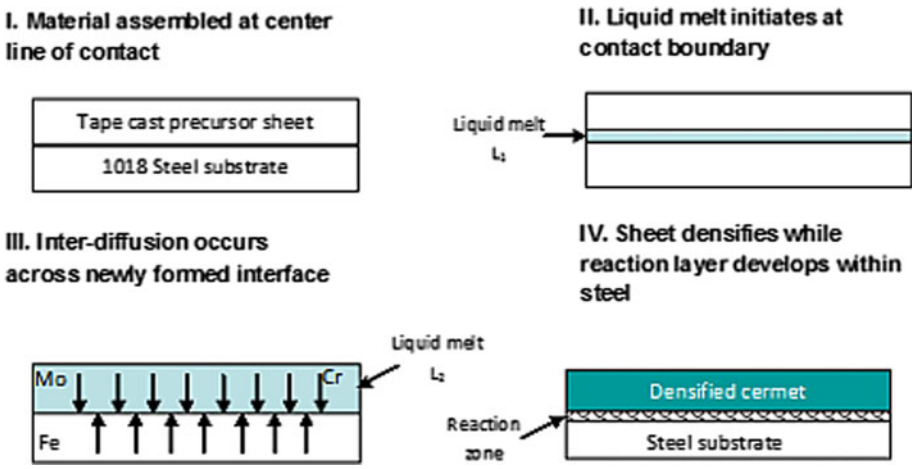

Fig. 13 Proposed mechanism for sinter bonding between 1018 steel and boride based cermets

It is evident that Mo signal is picked up from the complex boride phase and can be correlated to the locations X1 and X3 in the microstructures between Fig. 6 and 7. Fe being the major constituent in the continuous phase and also in the complex boride can be expected to have a continuous x-ray elemental map except regions of porosity and the results conform. The Fe and Mo distribution when compared with the actual microstructure suggests that Fe is picked up from both the binder phase and the complex boride phase, while Mo is lower and is observed from the boride precipitates in the case of both cermets. The dark regions correspond to porosity. Chromium is found to segregate in both Fe- and Mo-rich regions in the case of C50 cermet while it is found to segregate only in Fe-rich regions in the case of V30 cermet.

Precipitates of three different morphologies (Fig. 8) are observed, which are:

Liquid-rich FeB phase (x), which on solidification is observed as a networked structure due to the vaporization of polymer based binder.

MoB (y), which forms the neck with adjacent FeB particles.

Needle-shaped Mo_2FeB_2 (z), a complex boride phase responsible for the change in properties of these systems.

The x-ray spot spectra was obtained for C50 cermet sintered at 1000 °C as this temperature is marked with occurrence of newly formed phases.

The appearance of the liquid phases is congruent with the shrinkage observed in the thickness direction. Subsequently, a dense structure is obtained as temperature rises nearer to 1250 °C and corresponds with significant observed distortion. It is observed that the polymer binder is also completely removed when process is isothermally held at 400 °C.

The reactions which are occurring as inferred from the x-ray phase analysis data are

$$L_{1(\text{FeB rich})} + Fe + Mo + Cr + MoB \rightarrow Mo_2FeB_2 + Fe + \text{unreacted borides} \quad \text{(Eq 1)}$$

$$Mo_2FeB_2 + CrB + L_2 \rightarrow (Mo, Fe, Cr)_3B_2 + Fe_{(\text{matrix})} \quad \text{(Eq 2)}$$

$$Mo_2FeB_{2(\text{coarse})} + L_2 \rightarrow Mo_2FeB_{2(\text{fine})} + Fe_{(\text{matrix})} \quad \text{(Eq 3)}$$

Reaction (1) occurs in both cermets, while reaction (2) pertains C50 while V30 cermets follow reaction (3). Similar reactions have been reported in Ref 10 where it is to be noted

that Mo_2FeB_2 phase appears at 1126 °C. However from our x-ray diffraction data the phase has been identified at even lower temperature of 1000 °C. Reaction (3) is actually a representation of the solution-reprecipitation stage reported in liquid phase sintering (Ref 5). The configuration for bonding and the subsequent cermet bonded between two layers of steel is shown in Fig. 9. The layers of steel and densified cermet are easily distinguishable.

It can be inferred from the line scan analysis that Fe diffused from steel to cermet while Mo and Cr diffuses from cermet to the steel. These elements interact and constitute the reaction zone (Fig. 10, 11).

It can be noted that there is a localized crack at the interface for the V30 sample. This can arise owing to incomplete contact between precursor sheet and substrate and can be rectified by increasing the magnitude of the constant load during bonding. In Fig. 12, a higher magnification optical micrograph shows a homogenous defect free interface in the same sample.

Simultaneously occurring processes of sintering of the cermet and its bonding to the substrate through elemental diffusion is termed as sinter bonding. A reaction layer next to the interface is found to be a common feature in both grades of cermet. Diffusion of Fe from base metal constitutes the buildup of this layer. A mechanism has been proposed for the bonding process as depicted in Fig. 13.

Uniform bonding is observed owing to the coefficients of thermal expansion being similar (Ref 8). The interface thickness is found to increase in the periphery as compared to the center owing to surface tension assisting in liquid movement along the junction. Once a liquid melt "bridge" is established diffusion occurs through this pathway while the liquid front moves upward. In segment 3 of the model, inter-diffusion occurs concomitantly while liquid front propagates upward producing a densified cermet. It results in a densified cermet bonded onto the substrate.

The hardness variation across the multilayer is shown in Fig. 14. It can be observed that hardness increases at distances closer to the interface. A peak hardness of 980 $HV_{0.05}$ is observed in the complex borides while the binder phase showing a hardness of close to 200 $HV_{0.05}$ is obtained.

It can be observed that hardness is slightly higher in the reaction zone as compared to the substrate and drops to the value of substrate hardness as the region immediately adjacent to the interface is encountered. This suggests that the reaction zone is forming within steel.

4. Conclusions

The results show that upon sintering Mo_2FeB_2 phase starts appearing at 1000 °C which is expected to form due to the reaction between FeB rich liquid phase and the elemental constituents along with MoB imparting the characteristic hardness.

Sinter bonding with mild steel substrate via in situ formation of hard phases and densification of material was successfully performed.

Reaction layer was found to be a common feature in bonded material for both grades of cermet and is formed owing to the inter-diffusion of elements between substrate and cermet.

Acknowledgments

The authors are grateful to Prof. Ken-Ichi Takagi (Musashi Institute of Technology, Tokyo) and Dr. Hirofumi Tashiro (Toyo Kohan Co. Ltd., Japan) for their technical feedback and assistance. The assistance provided by Mr Ankit Jain, undergraduate student, IIT Kanpur with the experiments is also gratefully acknowledged.

References

1. K. Takagi, M. Komai, and S. Matsuo, Development of Ternary Boride Based Cermets, *Proc. Powder Metall. World Congr.*, 1994, **1**, p 227–234
2. Kohan's Hard Materials—KHM, Product Information Brochure, Toyo Kohan Co. Ltd, Tokyo, Japan
3. R. Thompson, The Chemistry of Metal Borides and Related Compounds, *Progress in Boron Chemistry*, Vol 2, R.J. Brotherton and H. Steinberg, Ed., Pergamon Press, Oxford, UK, 1970, p 173–230
4. K. Takagi, Development and Application of High Strength Ternary Boride Base Cermets, *J. Solid State Chem.*, 2006, **179**, p 2809–2818
5. R.M. German, *Liquid Phase Sintering*, Plenum Press, New York, NY, USA, 1985, p 1–94
6. K. Takagi, M. Komai, T. Watanabe, and Y. Kondo, Effect of Molybdenum and Carbon on the Properties of Iron Molybdenum Boride Hard Alloys, *Int. J. Powder Metall.*, 1986, **22**, p 91–96
7. R.M. German, K.S. Hwang, and D.S. Madan, Analysis of Fe-Mo-B Sintered Alloys, *Powder Metall. Int.*, 1987, **19**, p 15–18
8. K. Takagi, Y. Yamasaki, and M. Komai, High-Strength Boride Base Hard Materials, *J. Solid State Chem.*, 1997, **133**, p 243–248
9. K. Sivaraman, A. Griffo, and R.M. German, Novel Sinter Bonding Process to Coat Boride Cermets onto Steel Substrates for Wear Resistant Applications, *Adv. Powder Metall. Part. Mater.*, 1997, **2**, p 14.159–14.173
10. D. Rao and G.S. Upadhaya, Sintering of Mo_2FeB_2 Layered Cermet Containing SiC Fibers, *Mater. Chem. Phys.*, 2001, **70**, p 336–339
11. K. Takagi, S. Ohira, T. Ide, T. Watanabe, and Y. Kondo, New P/M Iron Containing Multiple Boride Base Hard Alloy, *Mod. Dev. Powder Metall.*, 1985, **16**, p 153–166
12. K. Sivaraman, A. Griffo, and R.M. German, Development of Ternary Boride Cermet for High Wear Resistant Applications, *Adv. Powder Metall. Part. Mater.*, 1996, **3**, p 11.67–11.80
13. B.D. Cullity, *Elements of X-ray diffraction*, Addison-Wesley Publishing Inc, Boston, MA, USA, 1978, p 10–555